Vital Surveillances

Changing Patterns of Epidemiological Characteristics and Spatial-Temporal Clusters of Human Brucellosis Based on County Level — China, 2011–2023

Shijian Zhou[1]; Huijie Qin[2]; Qingnan Shi[1]; Sihan Li[1]; Junyuan Chen[2]; Qiulan Chen[1,#]

ABSTRACT

Introduction: Human brucellosis persists as a critical public health challenge in China. Understanding disease clusters and trends is essential for implementing effective control strategies. This study evaluates the epidemiological characteristics and spatiotemporal distribution of brucellosis in China from 2011 to 2023.

Methods: Data were obtained from the National Notifiable Disease Reporting System (NNDRS). We conducted descriptive epidemiological analyses and employed SaTScan10.1 and ArcGIS10.7 software to identify disease clusters and generate county (district)-level incidence maps.

Results: The incidence of human brucellosis in Chinese mainland increased substantially between 2011 and 2023, rising from 38,151 cases (2.8/100,000) across 834 counties (25.4%) to 70,439 cases (5.2/100,000) across 2,290 counties (76.9%). A significant upward trend in reported incidence emerged during 2018–2023 (average annual percentage change (AAPC)=14.9%, P=0.01). Most cases (89.3%) occurred in individuals aged 25–69 years, with an increasing proportion among those aged over 60 years. While 96.1% of cases were reported in northern provincial-level administrative divisions (PLADs), southern regions demonstrated escalating incidence rates and expanding geographical spread. Southern PLADs exhibited a notable annual increase of 31.5% in reported incidence (P<0.01). Counties (districts) with incidence rates exceeding 10 per 100,000 expanded geographically from northwestern pastoral regions to southern areas and from rural to urban settings. Primary spatiotemporal clusters were concentrated in Inner Mongolia and adjacent provincial-level administrative divisions (PLADs), with emerging clusters identified in Yunnan, Guangdong, and Xizang.

Conclusions: The human brucellosis epidemic in China continues to intensify, characterized by rebounding incidence rates and broader geographical distribution across counties (districts). While spatiotemporal clusters remain predominantly centered in Inner Mongolia and neighboring regions, targeted interventions and increased resource allocation for high-risk areas and populations are imperative.

Brucellosis persists as one of the world's most significant "neglected zoonoses," presenting substantial threats to human health, livestock productivity, and socioeconomic stability (*1*). With an annual global incidence of approximately 2.1 million cases, predominantly concentrated in Africa and Asia, the disease continues to pose a major public health challenge (*2*). Despite China's successful suppression of human brucellosis during the 1990s through robust preventive and control strategies, the disease has experienced a marked resurgence in the 21st century, primarily driven by expansions in the livestock industry (*3*). Reported cases have increased dramatically, reaching an unprecedented peak of 70,439 in 2023. The geographic distribution of the epidemic has expanded substantially, extending beyond the traditional northwestern pastoral regions such as Inner Mongolia to encompass adjacent grassland and agricultural zones with high sheep and goat populations, as well as coastal and southeastern regions (*4*). This evolving epidemiological landscape necessitates a comprehensive delineation of current epidemic characteristics to enhance preventive and control measures.

Spatial-temporal cluster analysis of brucellosis serves as a crucial tool for identifying and prioritizing high-risk areas for targeted interventions. Current analytical approaches typically utilize provincial-level administrative divisions, predominantly focus on northern China, or examine only short-term trends

(4–5). A significant research gap exists regarding long-term spatial and temporal patterns of brucellosis at the more granular county (district) level nationwide. To address this knowledge gap, we conducted a comprehensive examination of the epidemiological patterns and spatial-temporal distribution of human brucellosis across Chinese mainland from 2011 to 2023.

METHODS

Human brucellosis surveillance data from 31 PLADs in China (2011–2023) were obtained from the National Notifiable Disease Reporting System (NNDRS). The system incorporated both clinically diagnosed and confirmed cases based on national health industry standards. Clinically diagnosed cases were defined as presumptive cases (those with epidemiological history and clinical manifestations) with positive screening test results, while confirmed cases were defined as presumptive or clinically diagnosed cases with confirmatory experimental evidence (5). We conducted descriptive analyses following established definitions for annual incidence (AI) and regional comparisons between southern and northern regions (3). Trend analyses employed Joinpoint regression models to calculate the average annual percentage change (AAPC). Statistical analyses and disease data visualization were performed using SAS (version 9.4, SAS Institute Inc., Cary, USA) and ArcGIS Desktop (version 10.6; Esri; Redlands, California, USA).

For spatiotemporal cluster identification, we employed a Poisson retrospective spatiotemporal scan statistic using SaTScan^{TM} software developed by Kulldorff (5). The analysis utilized a discrete Poisson distribution model to examine high spatial clustering areas across the Chinese mainland. Each scanning window was evaluated using log-likelihood ratio (LLR) and relative risk (RR) calculations to test hypotheses. The window with the maximum LLR was designated as the primary cluster, while other statistically significant windows were classified as secondary clusters (4). The analysis was conducted at the county level with daily temporal precision. The temporal aggregation period was set to 14 days, corresponding to the brucellosis incubation period. Maximum spatial and temporal window sizes were configured to encompass no more than 5% of the at-risk population

and 50% of the study duration, respectively.

RESULTS

Sociodemographic Characteristics

From 2011 to 2023, the Chinese mainland reported 656,628 cases of human brucellosis across 31 PLADs. Males were disproportionately affected, with a male-to-female ratio of 2.6∶1 (475,706 males versus 180,922 females). The mean age of affected individuals was 47.59±14.41 years, with 89.3% of cases occurring in those aged 25–69 years. A notable demographic shift emerged over the study period: the proportion of cases in individuals over 60 years increased annually, while the proportion in those aged 15–29 years showed a consistent decline, resulting in a net demographic shift of 7%. Throughout the study period, agricultural workers and herders constituted the predominant occupational groups affected, accounting for 82.7% to 89.7% of all cases.

Temporal Trend and Seasonality

The nationwide incidence of brucellosis demonstrated marked fluctuations throughout the study period. Reported cases increased substantially from 38,151 (2.8/100,000) in 2011 to 70,439 (5.2/100,000) in 2023, with a mean annual incidence of 3.66 per 100,000. Peak incidence occurred in 2023 at 5.0 per 100,000. A significant upward trend was observed from 2018 to 2023 (AAPC=14.9%, P=0.01). Southern PLADs exhibited a particularly steep increase in reported incidence from 2011 to 2023 (AAPC=31.5%, P<0.01). The disease demonstrated clear seasonal patterns, with 54.3% of annual cases occurring between March and July.

Spatial Characteristics

From 2011 to 2023, PLADs in northern China accounted for 96.1% of total brucellosis cases. However, PLADs in southern China exhibited a marked increase in reported cases, rising from 0.6% in 2011 to 7.4% in 2023. During this period, the geographic distribution of affected counties (districts) expanded substantially, from 834 (25.4%) in 2011 to 2,290 (76.9%) in 2023. In southern China specifically, the number of affected counties (districts) increased nearly fourfold, from 96 (9.0%) in 2011 to 932 (40.7%) in 2023 (Figure 1). Counties (districts) reporting high incidence rates exceeding 100 per 100,000 population increased from 44 (1.5%) in 2011
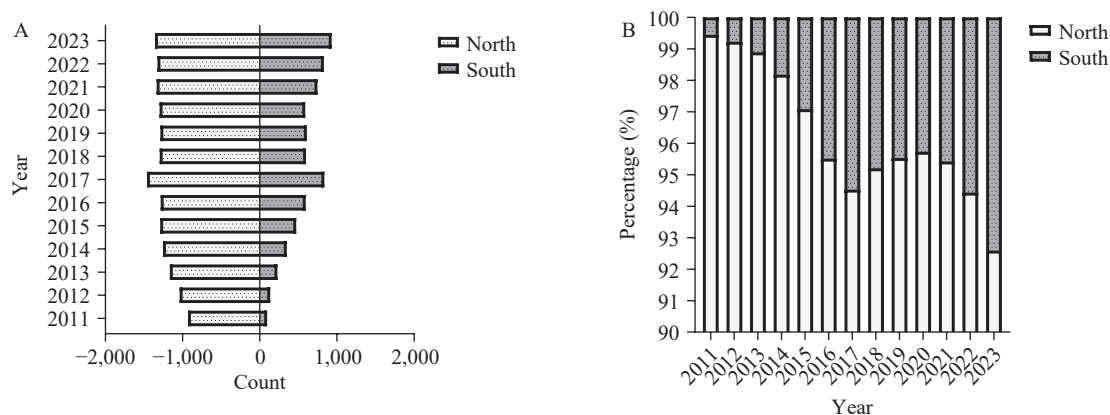
FIGURE 1. Human brucellosis in northern and southern China, 2011–2023. (A) Number of affected counties; (B) Proportion of reported cases.

to 71 (2.4%) in 2023, predominantly concentrated in northern regions, particularly Inner Mongolia and Xinjiang. Similarly, counties (districts) with incidence rates greater than 10 per 100,000 showed substantial expansion, increasing from 247 (8.4%) in 2011 to 525 (17.6%) in 2023. The geographic spread of brucellosis has demonstrated a consistent southward progression from northern China since 2013 (Figure 2 and Supplementary Table S1, available at https://weekly.chinacdc.cn/)

Spatial Clustering Analysis

From 2011 to 2023, we identified 227 spatiotemporal clusters of human brucellosis, comprising 13 primary and 214 secondary clustering areas. The primary clusters initially centered in eastern Inner Mongolia before progressively expanding to encompass eight adjacent PLADs (Heilongjiang, Jilin, Liaoning, Hebei, Shanxi, Shaanxi, Ningxia, Gansu) and part regions in Xinjiang. This expansion pattern persisted throughout the study period. Notably, in 2015–2016, novel clusters emerged in southern PLADs, specifically affecting Guangdong, Hubei, and Guangxi (Supplementary Tables S2–S3, available at https://weekly.chinacdc.cn/). By 2017, the disease had spread to 183 counties (districts), predominantly concentrated in northern PLADs including Shanxi, Inner Mongolia, Heilongjiang, Xinjiang, Hebei, Liaoning, Gansu, and Shandong, with Xizang reporting secondary clusters for the first time (Supplementary Tables S2–S3). The period between 2018 and 2021 saw a reduction in affected counties, with clusters reconcentrating in Inner Mongolia and adjacent PLADs. While clusters in Yunnan persisted from 2019 onward, Xinjiang ceased reporting clusters

from 2020. Re-emergence of spatiotemporal clusters in Xinjiang in 2023. In 2022–2023, there was a resurgence in affected counties, primarily in the Inner Mongolia and its surrounding eight PLADs, as well as in Shandong, Henan, Qinghai, and Xinjiang PLADs. The temporal evolution of primary clustering showed distinct geographical shifts: from 2011 to 2014, it was predominantly in eastern Inner Mongolia and neighboring PLADs such as Heilongjiang and Jilin; from 2015 to 2017, it shifted to the western Inner Mongolia and expanded to Xinjiang, Ningxia, and other regions; from 2018 to 2021, it returned to eastern Inner Mongolia; from 2022 to 2023, shifted to western Inner Mongolia as well as Shanxi, Shaanxi, Ningxia, Gansu, Qinghai and Xinjiang regions (Figure 3). Among the 227 spatiotemporal clusters identified, primary clusters occurred predominantly from February to August, while secondary clusters spanned January to July (Table 1).

DISCUSSION

This study reveals significant shifts in the epidemiological landscape and spatiotemporal distribution of brucellosis across China from 2011 to 2023. Our findings demonstrate the persistent severity of the epidemic, characterized by both a resurgence in reported cases and substantial geographic expansion across counties (districts). The disease pattern has evolved from its initial concentration in northern pastoral provinces to encompass adjacent grassland and agricultural regions, ultimately extending into southern coastal and southwestern areas. Spatiotemporal analysis revealed distinct clustering patterns, with primary hotspots centered in Inner Mongolia and traditional
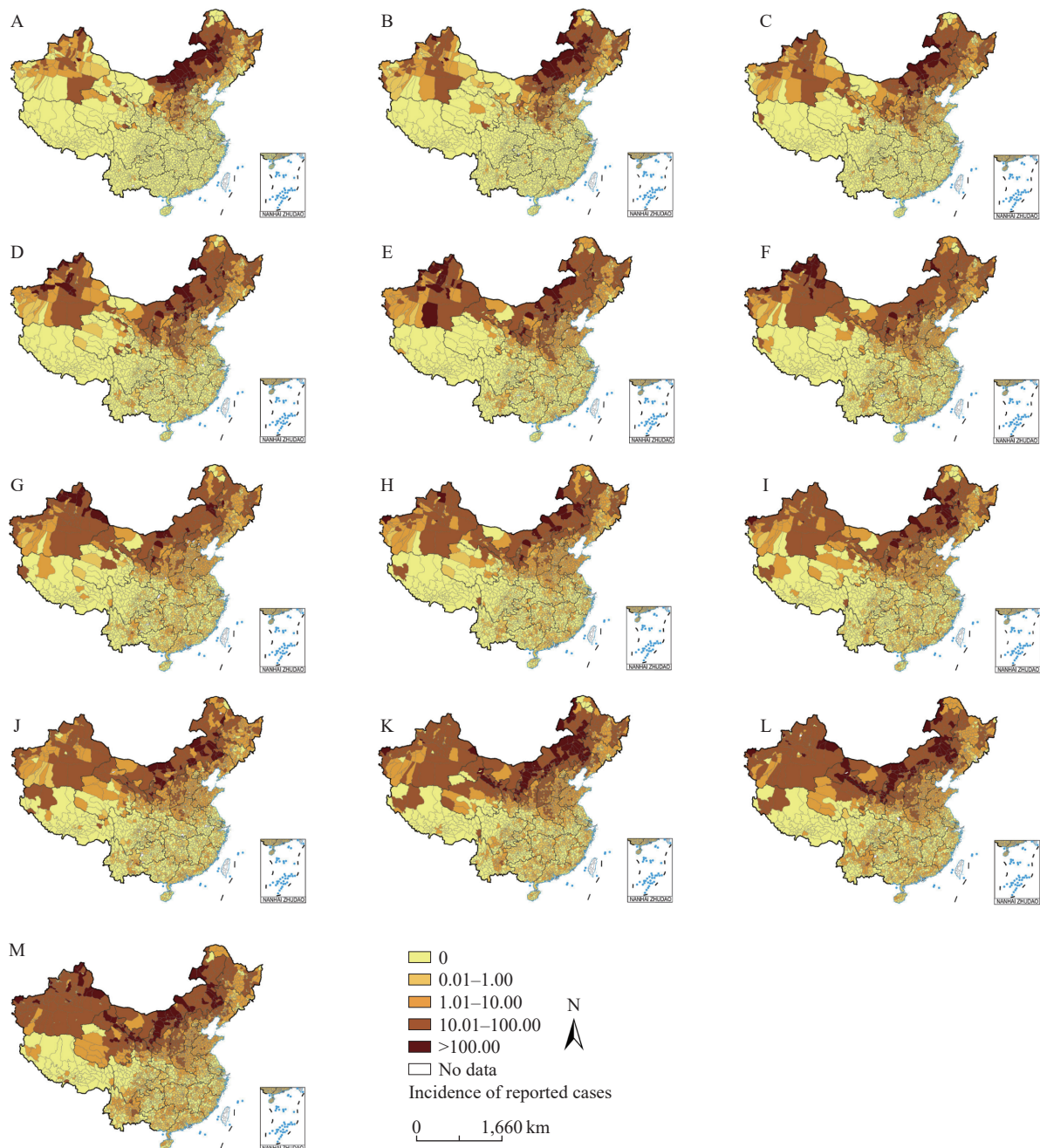
FIGURE 2. Geographical distribution of incidence of the reported human brucellosis in 31 PLADs of China, 2011–2023. (A)–(M) From 2011 to 2023.
Abbreviation: PLAD=provincial-level administrative division.
Map approval number: GS 京 (2025)0527 号.

pastoral regions of western and northeastern China. Throughout the 13-year study period, the disease exhibited a clear eastward-to-westward progression within Inner Mongolia, subsequently spreading to adjacent PLADs and part regions in Xinjiang. A particularly noteworthy development since 2019 has been the emergence of new hotspots in the southern PLAD of Yunnan, demanding immediate attention from public health authorities. In 2023, many hotspots appeared in Xinjiang and Qinghai, which may be related to its improved ability to detect brucellosis.

The age distribution analysis reveals a concerning trend: the proportion of infections among individuals over 60 years has shown consistent annual increases. This demographic shift likely reflects the aging population structure among Chinese farmers and
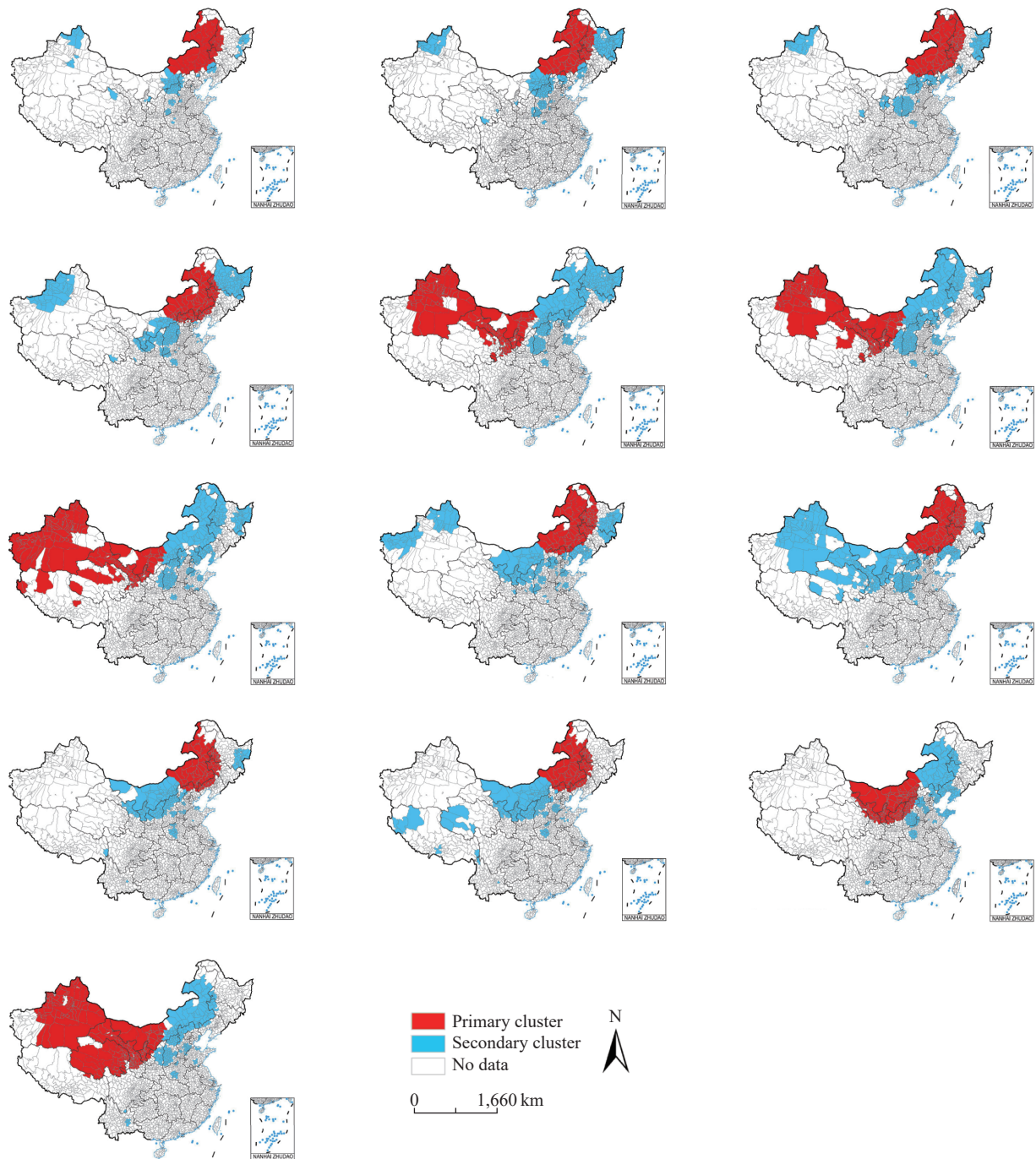
FIGURE 3. Spatial clustering of the reported brucellosis cases in 31 PLADs of China, 2011–2023. (A)–(M) From 2011 to 2023.
Abbreviation: PLAD=provincial-level administrative division.
Map approval number: GS 京 (2025)0527 号.

herders engaged in livestock management (5). This finding underscores the urgent need for targeted health education initiatives specifically designed for this vulnerable age group.

The rising incidence of human brucellosis in China, particularly in southern regions, can be attributed to several interconnected factors. First, there exists a robust positive correlation between human brucellosis incidence and livestock outbreak frequency (6–7). Despite persistent and intensifying animal outbreaks, preventive measures — including livestock vaccination programs and quarantine protocols — have proven

TABLE 1. Spatiotemporal clusters of human brucellosis in China, 2011–2023.

Scan time frame (year)	Cluster time (mm/dd–mm/dd)	Centroid (latitude, longitude)/ radius (km)	Cluster counties (n)	LLR	RR	P
2011	2/13–8/13	(48.6N, 116.8E)/715.6	78	16,848.2	15.2	<0.001
2012	1/31–7/30	(48.6N, 116.8E)/737.0	87	17,093.2	15.0	<0.001
2013	1/1–7/2	(48.6N, 116.8E)/780.7	104	11,305.8	10.2	<0.001
2014	1/1–7/2	(45.7N, 117.0E)/605.8	125	11,444.6	8.4	<0.001
2015	3/13–9/10	(43.5N, 95.0E)/1280.0	159	9,979.3	7.9	<0.001
2016	2/28–8/27	(43.5N, 95.0E)/1281.8	161	10,097.4	9.4	<0.001
2017	2/13–8/13	(48.3N, 87.2E)/2003.2	183	6,752.9	7.9	<0.001
2018	2/27–8/27	(48.6N, 116.8E)/809.3	117	9,690.0	11.1	<0.001
2019	2/13–8/13	(48.6N, 116.8E)/809.3	118	13,780.5	13.1	<0.001
2020	2/28–8/27	(45.7N, 118.8E)/530.6	109	14,367.6	13.5	<0.001
2021	1/30–7/30	(45.7N, 118.8E)/530.6	109	18,540.7	13.9	<0.001
2022	2/27–8/27	(41.5N, 106.4E)/644.0	159	24,912.4	15.3	<0.001
2023	2/27–8/27	(43.6N, 94.9E)/1312.2	223	20231.2	10.9	<0.001

Abbreviation: LLR=log likelihood ratio; RR=relative risk.

insufficient (4,8). Recent surveillance data indicate elevated seroprevalence rates among dairy cattle and sheep populations (9–10). Second, the surge in livestock product demand has intensified north-to-south animal transportation, exacerbating the epidemic's spread to southern regions (4,8). Third, inadequate regional quarantine measures and limited stakeholder awareness of quarantine protocols have contributed to outbreaks in southern China, as evidenced by cases linked to sika deer and raw goat milk consumption (11–12). Furthermore, the diversification of livestock production systems — encompassing free-range, grazing, and intensive production methods — has complicated disease prevention and control efforts (10,13).

The spatial-temporal clustering patterns of human brucellosis have aligned with broader epidemic trends, with Inner Mongolia and adjacent regions remaining critical focal points. Molecular epidemiological studies have revealed genetic homology between *Brucella* strains isolated from northern provinces, including Xinjiang and Inner Mongolia (14), and those found in Shanxi and neighboring provinces (15). This genetic relationship underscores the need for enhanced quarantine measures and stringent management of livestock and dairy product movement between high-incidence regions to curtail disease transmission. In Yunnan, the rapid emergence of brucellosis cases, potentially linked to expanding dairy goat operations, necessitates the implementation of prevention and control strategies specifically tailored to local livestock industry developments.

Despite the implementation of the National Brucellosis Prevention and Control Plan (2016–2020) (NBPCP), brucellosis incidence rates have continued their upward trajectory. In response, brucellosis was designated as a priority disease for prevention and control in 2022. This designation necessitates comprehensive animal-based prevention and control strategies from governmental bodies at all levels, encompassing immunization, quarantine, and culling protocols. Furthermore, there is an urgent need to strengthen occupational safety measures for at-risk populations to reduce both inter-animal transmission and occupational exposure, thereby mitigating the disease's escalating impact on human populations. Additionally, management approaches should be tailored to regional specificities, with enhanced oversight in high-risk areas. While this study presents a spatial-temporal aggregation analysis at the district-county scale, future research could explore patterns at smaller administrative levels, such as townships, to provide more granular insights for precise prevention and control strategies.

This study has several limitations. First, county codes for a small proportion (<10%) of cases could not be matched with the corresponding map dataset, though this discrepancy is minor and does not significantly impact the data's representativeness. Additionally, the reported case numbers may underestimate the true disease burden due to inherent limitations in surveillance data.

Corresponding author: Qiulan Chen, chenql@chinacdc.cn.

1 National Key Laboratory of Intelligent Tracking and Forecasting for Infectious Diseases, Chinese Center for Disease Control and Prevention, Beijing, China; 2 School of Public Health, Guangxi Medical University, Nanning City, Guangxi Zhuang Autonomous Region, China.

REFERENCES

1. Lai SJ, Chen QL, Li ZJ. Human brucellosis: an ongoing global health challenge. China CDC Wkly 2021;3(6):120 – 3. https://doi.org/10.46234/ccdcw2021.031.
2. Laine CG, Johnson VE, Scott HM, Arenas-Gamboa AM. Global estimate of human brucellosis incidence. Emerg Infect Dis 2023;29(9):1789 – 97. https://doi.org/10.3201/eid2909.230052.
3. Tao ZF, Chen QL, Chen YS, Li Y, Mu D, Yang HM, et al. Epidemiological characteristics of human brucellosis - China, 2016-2019. China CDC Wkly 2021;3(6):114 – 9. https://doi.org/10.46234/ccdcw2021.030.
4. Yang HM, Chen QL, Li Y, Mu D, Zhang YP, Yin WW. Epidemic characteristics, high-risk areas and space-time clusters of human brucellosis - China, 2020-2021. China CDC Wkly 2023;5(1):17 – 22. https://doi.org/10.46234/ccdcw2023.004.
5. Liang PF, Zhao Y, Zhao JH, Pan DF, Guo ZQ. Human distribution and spatial-temporal clustering analysis of human brucellosis in China from 2012 to 2016. Infect Dis Poverty 2020;9(1):142. https://doi.org/10.1186/s40249-020-00754-8.
6. Wang Y, Wang Y, Zhang LN, Wang AP, Yan Y, Chen YY, et al. An epidemiological study of brucellosis on Chinses mainland during 2004-2018. Transbound Emerg Dis 2021;68(4):2353 – 63. https://doi.org/10.1111/tbed.13896.
7. Zhang D, Lv DY, Zheng XJ, Duan R, Qin S, Lu XM, et al. Case report: screening and analysis for brucellosis in Akesai Kazak autonomous county, China. Am J Trop Med Hyg 2023;108(6):1201 – 3. https://doi.org/10.4269/ajtmh.22-0802.
8. Li Y, Tan D, Xue S, Shen CJ, Ning HJ, Cai C, et al. Prevalence, distribution and risk factors for brucellosis infection in goat farms in Ningxiang, China. BMC Vet Res 2021;17(1):39. https://doi.org/10.1186/s12917-021-02743-x.
9. Ran XH, Cheng JJ, Wang MM, Chen XH, Wang HX, Ge Y, et al. Brucellosis seroprevalence in dairy cattle in China during 2008-2018: a systematic review and meta-analysis. Acta Trop 2019;189:117 – 23. https://doi.org/10.1016/j.actatropica.2018.10.002.
10. Li LM, Wang Q, Shi JF, Li T, Zhao B, Ma QX, et al. Seroprevalence and potential risk factors of brucellosis in sheep from America, Africa and Asia regions: a systematic review and meta-analysis. Res Vet Sci 2023;165:105048. https://doi.org/10.1016/j.rvsc.2023.105048.
11. Tao ZF, Yang ZP, Chen YS, Yang SF, Xu JC, Wang Y, et al. Epidemiological survey of first human brucellosis outbreak caused by the sika deer (*Cervus nippon*) - Guizhou Province, China, 2019. China CDC Wkly 2021;3(14):301 – 3. https://doi.org/10.46234/ccdcw2021.081.
12. Di M, Tao ZF, Hua WP, Chen JD, Cao JM, Deng YQ, et al. Investigation of brucellosis caused by raw goat milk - Fujian Province, China, April-June, 2019. China CDC Wkly 2021;3(20):430 – 3. https://doi.org/10.46234/ccdcw2021.111.
13. An CH, Shen L, Sun MH, Sun YX, Fan SP, Zhao CX, et al. Exploring risk transfer of human brucellosis in the context of livestock agriculture transition: a case study in Shaanxi, China. Front Public Health 2022;10:1009854. https://doi.org/10.3389/fpubh.2022.1009854.
14. Zhang H, Deng XY, Cui BY, Shao ZR, Zhao XL, Yang Q, et al. Abortion and various associated risk factors in dairy cow and sheep in Ili, China. PLoS One 2020;15(10):e0232568. https://doi.org/10.1371/journal.pone.0232568.
15. An CH, Nie SM, Sun YX, Fan SP, Luo BY, Li ZJ, et al. Seroprevalence trend of human brucellosis and MLVA genotyping characteristics of Brucella melitensis in Shaanxi Province, China, during 2008-2020. Transbound Emerg Dis 2022;69(4):e423 – 34. https://doi.org/10.1111/tbed.14320.

SUPPLEMENTARY MATERIAL

SUPPLEMENTARY TABLE S1. Number of affected counties with different incidence levels in China, 2011–2023.

Year	Total number of counties	Incidence (1/100,000) of affected counties									
		0		0.01–1		1.01–10		10.01–100		100.01–	
		N	Prevalence (%)*	N	Prevalence (%)*	N	Prevalence (%)*	N	Prevalence (%)*	N	Prevalence (%)*
2011	2,958	1,932	65.31	372	12.58	407	13.76	203	6.86	44	1.49
2012	2,974	1,800	60.52	433	14.56	440	14.79	264	8.88	37	1.24
2013	2,935	1,543	52.57	505	17.21	540	18.40	314	10.70	33	1.12
2014	2,938	1,334	45.41	537	18.28	643	21.89	373	12.70	51	1.74
2015	2,946	1,184	40.19	611	20.74	711	24.13	397	13.48	43	1.46
2016	2,945	1,068	36.26	702	23.84	782	26.55	361	12.26	32	1.09
2017	2,948	1,005	34.09	802	27.20	813	27.58	309	10.48	19	0.64
2018	2,949	1,054	35.74	777	26.35	804	27.26	293	9.94	21	0.71
2019	2,947	1,049	35.60	742	25.18	815	27.66	309	10.49	31	1.05
2020	2,958	1,070	36.17	712	24.07	832	28.13	310	10.48	34	1.15
2021	2,976	893	30.01	721	24.23	845	28.39	452	15.19	65	2.18
2022	2,901	745	25.68	800	27.58	871	30.02	415	14.31	70	2.41
2023	2,978	688	23.10	803	26.96	962	32.30	454	15.25	71	2.38

Abbreviation: *N*=number of counties.

* Percentage of the counties.

SUPPLEMENTARY TABLE S2. Number of districts and counties involved in the primary clusters of brucellosis in China, 2011–2023.

Province	Year												
	2011	2012	2013	2014	2015	2016	2017	2018	2019	2020	2021	2022	2023
Inner Mongolia	41	45	51	55	22	24	25	54	55	48	48	56	29
Heilongjiang	31	32	41	13	0	0	0	44	44	21	21	0	0
Xinjiang	0	0	0	0	68	66	91	0	0	0	0	0	75
Gansu	0	0	0	0	43	45	38	0	0	0	0	26	54
Jilin	6	9	10	9	0	0	0	12	12	14	14	0	0
Ningxia	0	0	0	0	18	18	16	0	0	0	0	20	21
Liaoning	0	0	0	22	0	0	0	2	2	21	21	0	0
Hebei	0	1	2	25	0	0	0	5	5	5	5	0	0
Shanxi	0	0	0	0	0	0	0	0	0	0	0	35	0
Qinghai	0	0	0	0	7	7	9	0	0	0	0	2	42
Shaanxi	0	0	0	0	1	1	0	0	0	0	0	20	1
Xizang	0	0	0	0	0	0	4	0	0	0	0	0	1

SUPPLEMENTARY TABLE S3. Number of districts and counties involved in the secondary clusters of brucellosis in China, 2011–2023.

Province	Year												
	2011	2012	2013	2014	2015	2016	2017	2018	2019	2020	2021	2022	2023
Shanxi	53	78	87	97	93	116	96	62	89	51	53	48	79
Heilongjiang	17	76	51	107	121	93	93	47	17	36	0	20	9
Inner Mongolia	29	37	16	28	65	65	70	42	40	54	55	43	67
Hebei	16	28	32	9	51	38	71	50	37	31	43	73	63
Liaoning	7	13	19	0	18	16	46	70	73	0	0	68	4
Henan	3	7	13	25	25	19	11	7	17	37	37	36	24
Shandong	1	1	0	7	34	42	38	31	14	4	8	34	12
Xinjiang	12	20	21	42	0	0	0	49	68	0	0	0	0
Shaanxi	1	7	27	23	15	23	15	26	34	20	20	0	21
Gansu	0	0	1	18	0	0	0	18	48	14	15	0	0
Ningxia	2	1	8	18	0	0	0	20	19	20	20	0	0
Jilin	0	1	2	3	17	11	12	10	0	0	0	10	7
Qinghai	1	2	2	1	0	0	0	0	23	0	3	0	0
Beijing	0	2	3	0	2	2	1	2	2	1	0	1	0
Xizang	0	0	0	0	0	0	0	0	0	1	9	0	0
Yunnan	0	0	0	0	0	0	0	0	1	1	2	3	6
Tianjin	0	0	1	0	0	1	1	0	0	0	0	0	0
Guangdong	0	0	0	0	1	0	0	0	1	0	0	0	0
Hubei	0	0	0	0	0	1	0	0	0	0	0	0	0
Guangxi	0	0	0	0	0	1	0	0	0	0	0	0	0
Sichuan	0	0	0	0	0	0	0	0	0	0	0	0	1